ELSEVIER

Separations Technology 6 (1996) 43–54

Separations Technology

Analysis of the sodium lactate concentration process by electrodialysis

Nicoletta Boniardi, Renato Rota*, Giuseppe Nano, Bruno Mazza

Dipartimento di Chimica Fisica Applicata, Politecnico di Milano, Via Mancinelli, 7, 20131 Milano, Italy

Received 4 August 1995; accepted 25 November 1995

Abstract

Electrodialysis is an interesting technique developed for recovering and purifying salts and acids from fermentation broths. In this work the concentration process of sodium lactate solutions was analyzed using a two-compartment electrodialytic unit equipped with commercial membranes (Neosepta AMX and CMX, Tokuyama Soda). The influence of several operating parameters on the overall process performance was investigated. For instance, it came out that at low current density values such membranes are able to operate a perfect separation of opposite charges, resulting in a good process performance. Moreover, water transport by electro-osmosis has to be considered, hence lowering the stack performance. Lastly, the reliability of a general mathematical model for this process was tested. The consistency between experiments and model results is fairly good, allowing the use of this model for design and optimization purposes.

Keywords: Electrodialysis; Membranes; Sodium lactate; Modeling

1. Introduction

As an industrial process, the production of organic acids (e.g. acetic, citric, malic, and lactic acid) through fermentation has become increasingly important in recent years [1–3]. The main problem of the process is that fermentation-derived acids are often difficult and expensive to purify. This is especially true when substances such as cheese-whey or molasses are used as the starting material. These substances contain many impurities thus requiring the use of several purification procedures in order to obtain commercial grade products. Among the purification processes considered, electrodialysis has been found potentially useful in the isolation and the purification of organic acids from fermentation media. Specifically, it can be used to recover and concentrate the salable product from the fermentation broth, or for recycling nutrients and microbial cells back to the reactor [3–5]. Electrodialysis may even control the pH of the fermentation broth without adding a neutralizer. Moreover, it has been demonstrated that the isolation of lactic acid during fermentation by electrodialysis enhances the productivity. In other words, electrodialysis is also able to reduce the inhibitory effect of a microbial metabolic product on microbial metabolism, thus increasing the process yield [6–8].

In particular, the production of lactic acid is growing due to its great potential in manufacturing biodegradable packaging and films [9]. In this case, electrodialysis has been used in different separation and purification procedures involving both conventional electrodialysis to concentrate lactate salts [4,10] or to recover lactic acid from fermentation broth [11–13], and water splitting electrodialysis to convert lactate salts into lactic acid [14].

The performance of a four-compartment electrodialytic stack for the recovery of lactic acid from sodium lactate has been discussed elsewhere [15]; the present work is concerned with the use of electrodialysis as a

---

* Corresponding author, Fax: +39 2 23993180; E-mail: ROTA@IPMCH2.POLIMI.IT.

PII:S0956-9618(96)00139-W

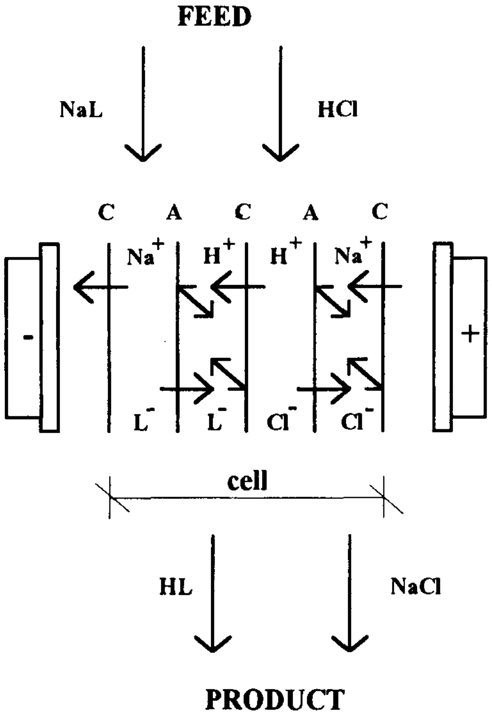

Fig. 1. Sketch of a four-compartment cell stack. C and A indicate cation- and anion-exchange membranes, respectively.

preliminary stage in downstream processing of lactic acid production by fermentation. In particular, the performance of a two-compartment cell stack for concentrating sodium lactate solutions was examined. Several experiments were carried out in order to investigate the effects of several operating parameters on the overall process performance, and a mathematical model was developed for simulating the experimental results.

2. Materials and methods

The electrodialysis unit (Eurodia, TS-EUR2-5 D) used for all the experiments consisted of an alternating series of commercial anion- and cation-selective membranes separated by flow distribution gaskets. The membrane stack was located between an anolyte and a catholyte compartment. Electrode chambers respectively contained a platinum-plated titanium anode and a stainless steel cathode. The electrodialyzer was equipped with ten anion-exchange membranes (Neosepta AMX, Tokuyama Soda) and 12 cation-exchange ones (Neosepta CMX, Tokuyama Soda), arranged to give five cells based on a four-compartment configuration (see Fig. 1); the total working surface was equal to 0.44 m^2.

The general flowsheet of the process involved five independent streams: the electrode feed solution was provided by the same stream line to both electrode compartments, while the remaining four distribution circuits fed the diluted and the concentrated compartments. Each solution came from a storage tank, passed through a pump, a rotameter, a cell compartment, and then flowed back to the tank in a batch recirculation operation mode. Solution flow rate was 0.3 l/min for each compartment. Moreover, each reservoir was equipped with a refrigerating coil to maintain a constant temperature of the solutions (see Fig. 2).

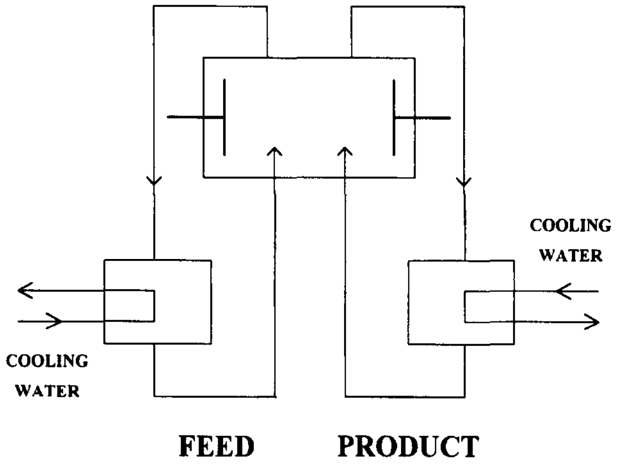

Fig. 2. Batch recirculation operation mode.

In this work, the circuit configuration was modified to convert the electrodialysis stack into the two-compartment unit (with ten cells) shown in Fig. 3.

The electrodialyzer was equipped with a power supply from Nemic Lambda (PWS 350-35). This instrument allowed the setting of either the voltage (0 ÷ 35 V) or the current (0 ÷ 10 A).

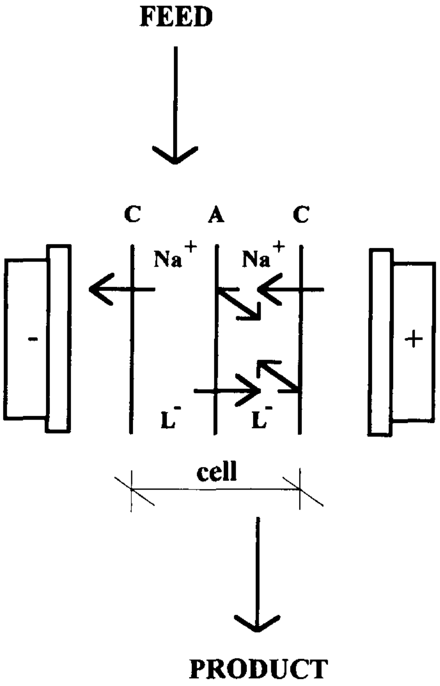

Fig. 3. Sketch of a two-compartment cell stack. Legend as in Fig. 1.

Feed solutions of sodium lactate used in all the experiments were prepared by diluting a commercial solution (analytical grade, purity > 99%) with distilled water up to the required concentration. An aqueous solution of sodium chloride (0.5 N) was used to feed the electrode compartments.

Sodium lactate concentration was measured using a gas-chromatograph equipped with FID and Carbopack B-DA-4% Carbowax 20 M (2 m × 2 mm i.d.) column.

3. Experimental results and discussion

All the experiments were carried out at a solution temperature of 20°C, and operated with a batch recirculation mode as shown in Fig. 2. In this operation mode, both the feed and the product streams were recycled to the electrodialysis stack from two separate tanks.

A few preliminary tests were performed to investigate the extent of both the solvent and solute permeation through the membranes with no electrical field applied. This was done by circulating the solutions without operating the power supply. In particular, the enriched compartments were fed with distilled water, while a sodium lactate solution was used as the diluted stream. Three different runs, using solutions with sodium lactate concentrations equal to approximately 40, 60 and 90 g/l, were carried out by circulating the solution for about 4 h. Both the volume of the solutions in the reservoirs and the sodium lactate concentration in the enriched tank were measured.

For the runs carried out with low sodium lactate concentration, no volume variations were observed. Moreover, no sodium lactate was detected in the concentrated tank. For the experiment performed at 90 g/l, whereas no salt was found in the concentrated tank, the final volumes of the solutions in each reservoir were found to be slightly different from their initial value as shown in Fig. 4 (see curve labeled control). It is reasonable to assume that solute and water permeation through the membranes was quite negligible.

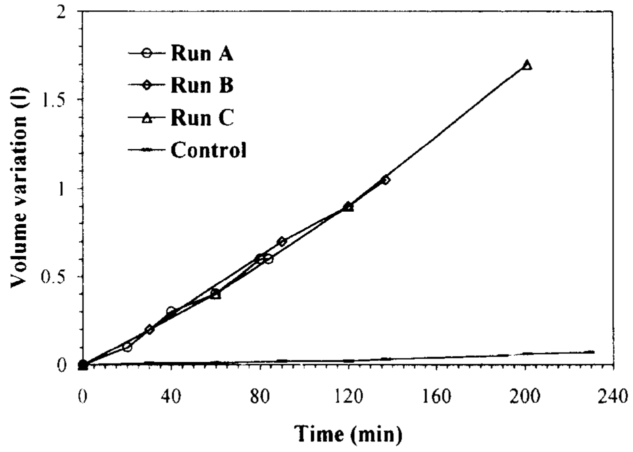

Fig. 4. Tank volume variations versus time for runs A–C carried out at the same current density. Control run results (i = 0 A/m^2 and C_{in} = 90 g/l) are also reported. See Table 1 for run labels.

Additional experiments were performed to investigate the electro-transport phenomena. All the runs were carried out by feeding the stack with sodium lactate solutions, and supplying a constant current value. In this case, the concentration of sodium lactate in the concentrated stream was found to increase, while that of the diluted stream decreased accordingly. Each run was carried out until the concentration of the diluted stream required a voltage value exceeding 35 V (that is, the maximum value attainable by the power unit) in order to sustain the given current value.

The performance of the process was examined for feed solutions of different concentrations and at different current density values. To investigate the effect of the initial concentration, three runs at the same current density were carried out, whereas the effect of the current density was studied in three experiments performed at similar initial concentration of sodium lactate (see experimental conditions summarized in Table 1). Moreover, in order to determine the experimental accuracy, repeated runs were made (runs E and Er). Fig. 5, which gives the tank volume variation and the stack voltage for these two runs, shows the good reproducibility of the experimental procedure. This was also confirmed by the overall mass balance for the solute (with an average error of 10% for all the experimental runs).

Experimental results are summarized in Table 2 which gives the volume and concentration of the solutions in the reservoirs and the overall stack voltage. The same data are also presented in Figs. 4, 6, 7, and 8.

In Fig. 6, the sodium lactate equivalents transferred versus time are shown. The data indicate that the initial concentration of sodium lactate has no effect on the rate of the electro-transport. Obviously, higher salt concentration corresponds to an increase in the run duration time. For this reason it is possible to compare the run performed at 50 g/l of sodium lactate with the one carried out at similar initial concentrations (60 g/l). The experimental results obtained at different current densities are summarized in Fig. 7. These results lead to a similar conclusion: namely, the highest value of current density corresponds to the shortest duration time. Moreover, the rate of sodium lactate migration through the membranes increases in proportion to the current density.

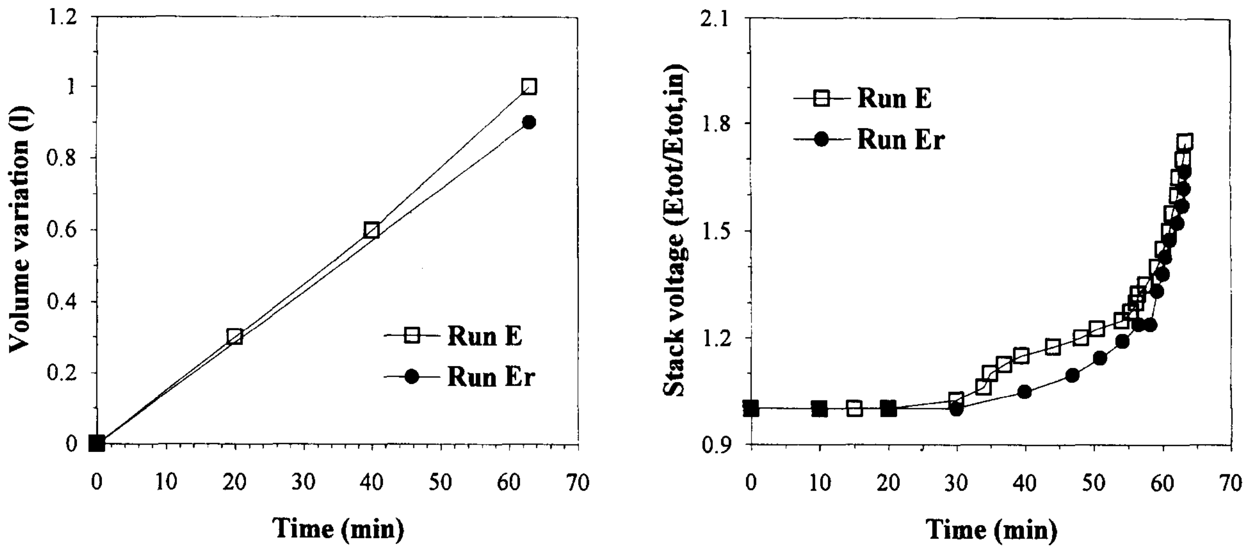

Fig. 5. Comparison between experimental runs E and Er. Stack voltage is made dimensionless dividing by the initial value. See Table 1 for run labels.

In addition to the movement of ionized species, water associated with the ions was also transported through the membranes. This phenomenon, called electro-osmosis, is shown in Figs. 4 and 8 where the volume variations in both the reservoirs versus time are displayed. The volume of the concentrated solution increases, while that of the diluted one decreases accordingly. It can be seen that the volume variation is proportional to the current density, that is, to the ion flow rate through the membranes, while the initial feed concentration has no influence on the rate of water transport. In the same figures, the experimental data are compared to those obtained with no current applied (curve labeled control); it is evident that water permeation under such a condition is negligible.

The overall process performance may be described by the sodium lactate recovery (L.R.), the current efficiency (C.E.), the specific energy requirement (S.E.R.), and the average power requirement (P.R.). The definitions of these performance indexes are given below, together with a brief discussion concerning their determination.

The sodium lactate recovery indicates the percentage of salt recovered from the feed solution. It can be easily computed as the ratio between the amount of sodium lactate transferred from the diluted to the concentrated tank during the run ($\mathrm{NaL_{in}}$-$\mathrm{NaL_{fin}}$) and the amount of sodium lactate present in the diluted reservoir at the beginning ($\mathrm{NaL_{in}}$):

$$\mathrm{L.R.} = \frac{(\mathrm{NaL_{in}} - \mathrm{NaL_{fin}})}{\mathrm{NaL_{in}}} \cdot 100 \qquad (1)$$

Values of L.R. close to 100% mean that almost all the salt in the feed solution can be recovered.

The current efficiency is given by the ratio between the number of sodium lactate equivalents recovered from the feed solutions (($\mathrm{NaL_{in}}$-$\mathrm{NaL_{fin}}$)/EW, where EW is the equivalent weight of sodium lactate) and that computed from the electric charge passed through

Table 1
Scheme of the experimental runs

C_{in}	i (A/m^2)		
(g/l)	110	200	400
40		A	
50	D		
60		B	E, Er
90		C	

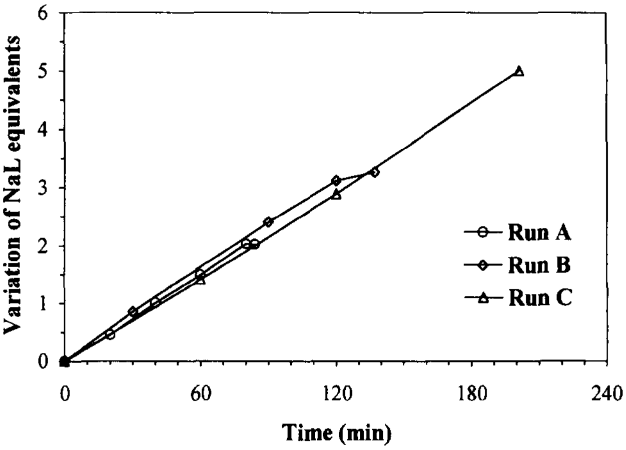

Fig. 6. Variation of equivalent number in the reservoirs versus time for runs, A–C carried out at the same current density. See Table 1 for run labels.

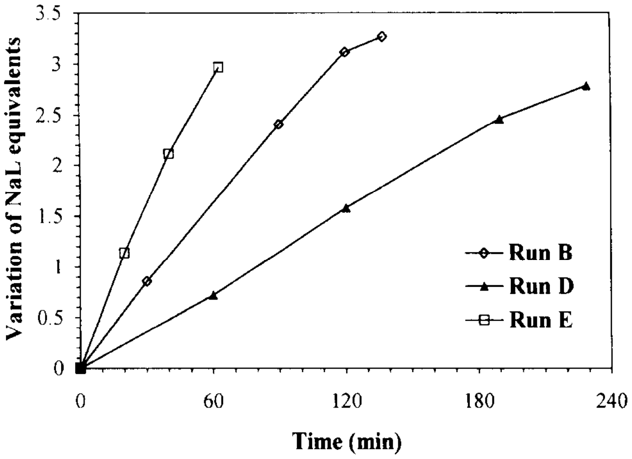

Fig. 7. Variation of equivalent number in the reservoirs versus time for runs B, D and E carried out at similar initial concentration values. See Table 1 for run labels.

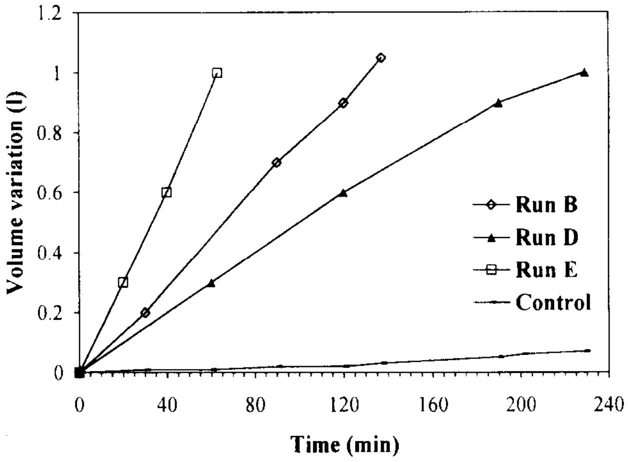

Fig. 8. Tank volume variation versus time for runs B, D and E carried out at similar initial concentration values. Control run as in Fig. 4. See Table 1 for run labels.

the stack:

$$\text{C.E.} = \frac{\Delta \text{equiv}_{\text{exp}}}{\Delta \text{equiv}_{\text{th}}} = \frac{\left(\dfrac{\text{NaL}_{\text{in}} - \text{NaL}_{\text{fin}}}{\text{EW}}\right)}{\dfrac{(I \cdot n_{\text{c}} \cdot t_{\text{fin}})}{F}} \cdot 100 \qquad (2)$$

Here NaL_{in} and NaL_{fin} represent, respectively, the initial and final amount of sodium lactate in the feed reservoir (that is, the diluted one), $\Delta\text{equiv}_{\text{exp}}$ and $\Delta\text{equiv}_{\text{th}}$ are the experimental and theoretical variations of equivalents in the same tank, I is the current, n_{c} the number of cells, t_{fin} the run duration time, and

Table 2
Volume and concentration of the solutions in the reservoirs, and stack voltage measured in all the experimental runs. Subscripts c and d refer to concentrated and diluted tank, respectively. See Table 1 for run labels.

Run	Time (min)	V_c (l)	V_d (l)	C_c (g/l)	C_d (g/l)	Voltage (V)
A	0	6.3	6.4	38	37	12.0
	20	6.4	6.3	46	30	13.0
	40	6.6	6.1	50	21	13.0
	60	6.7	6.0	62	13	14.0
	80	6.9	5.8	69	3	21.0
	84	6.9	5.8	68	2	35.0
B	0	6.2	6.2	62	62	11.0
	30	6.4	6.0	77	50	12.0
	60	6.6	5.8	90	31	12.3
	90	6.9	5.5	95	21	13.0
	120	7.1	5.3	103	6	15.0
	137	7.2	5.1	104	3	35.0
C	0	6.3	6.3	90	89	11.0
	60	6.7	5.9	109	69	11.5
	120	7.2	5.4	124	36	12.5
	201	7.8	4.6	146	2	35.0
D	0	6.0	6.0	52	52	7.5
	60	6.3	5.7	62	40	8.0
	120	6.6	5.4	75	26	8.5
	190	6.9	5.1	86	8	10.0
	229	7.0	5.0	90	1	35.0
E	0	6.6	6.3	58	61	20.0
	20	6.9	6.0	76	45	20.0
	40	7.2	5.7	87	27	23.0
	63	7.6	5.3	95	18	35.0
Er	0	6.0	6.0	57	58	21.0
	63	6.9	5.1	92	7	35.0

F the Faraday constant. The more efficient the separation of ions of opposite charge performed by the ion-selective membranes, the closer to 100% the current efficiency.

The specific energy requirement is the amount of electric energy required to recover one gram of sodium lactate from the feed solution:

$$\text{S.E.R.} = \frac{\int_0^{t_{\text{fin}}} (I \cdot E_{\text{tot}}) \cdot dt}{\text{NaL}_{\text{in}} - \text{NaL}_{\text{fin}}} \tag{3}$$

where E_{tot} is the overall stack voltage and t the time. Since both E_{tot} and I can change during a run (depending on the power supply conditions), the integral in Eq. 3 has to be evaluated numerically on the basis of suitable experimental (or computed) data.

Finally, the average power requirement during a run can be computed as the ratio between the energy requirement and the run duration time:

$$\text{P.E.} = \frac{\int_0^{t_{\text{fin}}} (I \cdot E_{\text{tot}}) \cdot dt}{t_{\text{fin}}} \tag{4}$$

The experimentally determined values of these quantities are shown in Figs. 9 and 10. It can be seen that the sodium lactate recovery is almost independent on both the feed solution concentration and the current density. It is possible to recover more than 95% of the initial sodium lactate in all the cases studied, except the run performed at current density equal to 400 A/m^2. The current efficiency is found to be greater than 95% for all the runs. The specific energy and the power requirement increase with the current density.

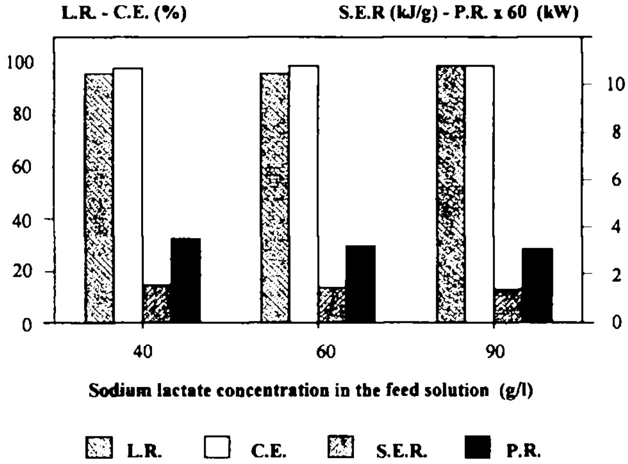

Fig. 9. Process performance indexes for runs A–C carried out at the same current density. L.R. is the sodium lactate recovery (Eq. 1), C.E. the current efficiency (Eq. 2), S.E.R. the specific energy requirement (Eq. 3), and P.R. the average power requirement (Eq. 4) which is multiplied by 60. See Table 1 for run labels.

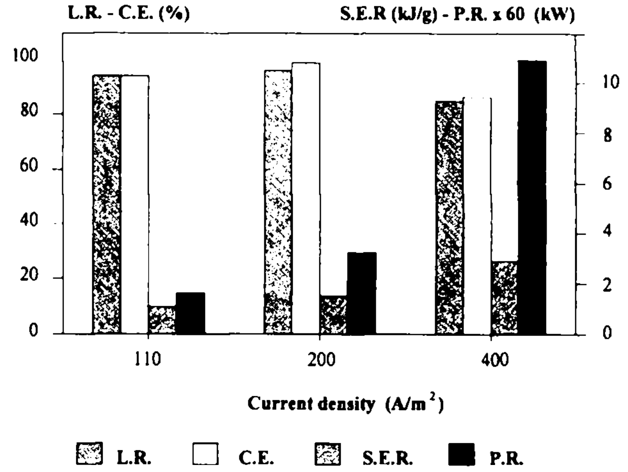

Fig. 10. Process performance indexes for runs B, D and E carried out at similar initial concentration values. Legend as in Fig. 9.

Fig. 9 shows that the specific energy requirement appears to decrease slowly with the increase of the initial concentration. The average power requirement exhibits a similar behavior. For experiments performed with solutions of the same initial concentration, the power requirement depends strongly on the current density (see Fig. 10).

4. Mathematical modeling

In a previous work [16] a general mathematical model capable of representing the main features of an electrodialysis unit was developed and validated by comparisons with experimental results concerning the recovery of lactic acid from sodium lactate solutions.

The main purpose of this section is to discuss such a model for the special case of a two-compartment stack and to verify its applicability to situations different from those used in the model formulation. In particular, the original model was based on experimental data collected from a four-compartment unit fed with four different solutions (namely, sodium lactate, lactic acid, hydrochloric acid and sodium chloride), whereas the present work was conducted using a two-compartment unit fed by sodium lactate solutions.

Assuming that the solute concentration inside each compartment (apart from the boundary layers adjacent to the membranes, as shown in Fig. 11) is uniform and the density of the solution is constant, the mass balance equation for the solute in the kth compartment ($k = c$ or d, i.e. concentrated or diluted) is:

$$V_{\text{comp},k} \cdot \frac{dC_k}{dt} = Q_k^0 \cdot C_k^0 - Q_k \cdot C_k + J_k \tag{5}$$

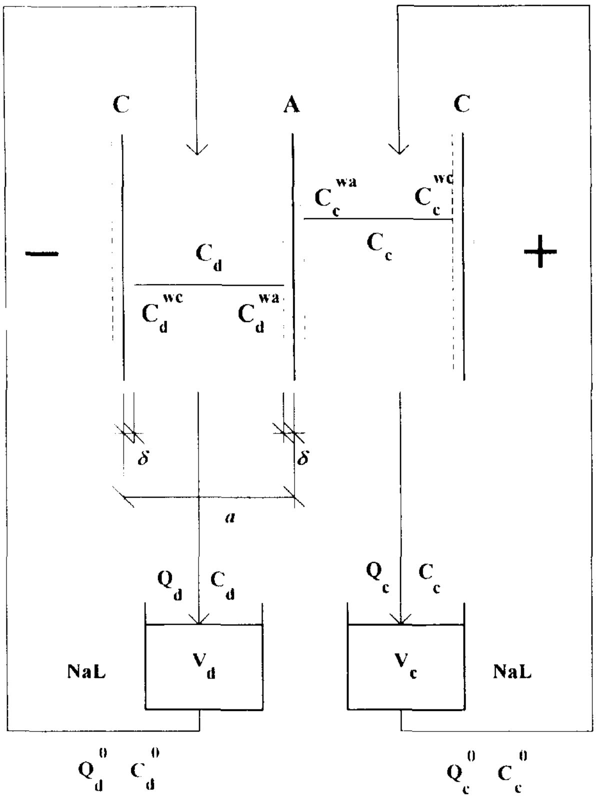

Fig. 11. Cell model.

Here $V_{\mathrm{comp},k}$ is the volume of either the diluted ($k=d$) or concentrated ($k=c$) compartment of the stack; C_k and C_k^O are, respectively the solute concentration inside the kth compartment (which is equal to that leaving the same compartment) and the solute concentration entering the kth compartment (see Fig. 11); analogously, Q_k and Q_k^O are the flow rates of the solution leaving and entering the kth compartment; lastly, J_k is the net flux of solute entering the kth compartment through the membranes.

It should be noted that the assumption of uniform concentration inside each compartment is usually quite reasonable. Even if the compartment is enlarged, the presence of turbulence promoters between the membranes prevents the formation of concentration gradients in the direction perpendicular to the membranes. Moreover, the solute concentration can be approximated as uniform also in the flow direction (parallel to the membranes) as far as the solute flux through the membrane is much lower than that entering the compartment:

$$J_k << Q_k^0 \cdot C_k^0 \tag{6}$$

This could be questionable only for the final part of the run, where the solute concentration in the diluted reservoir approaches zero. However, a comparison between the results of this simplified model and those of a more complex one (which accounts also for concentration gradients in the flow direction) confirmed that the assumption of uniform solute concentration is correct for all the cases here investigated.

The overall mass balance of the solution is:

$$Q_k^0 - Q_k + N_{\mathrm{wk}} = 0 \tag{7}$$

where N_{wk} is the net flux of water entering the kth compartment through the membranes.

Assuming the reservoirs well stirred, the mass balance equation for the solute in the kth reservoir is:

$$\frac{d(C_k^0 \cdot V_k)}{dt} = n_c \cdot (Q_k \cdot C_k - Q_k^0 \cdot C_k^0) \tag{8}$$

Here V_k is the volume of the kth reservoir and n_c the number of cells.

The mass balance relationship for the solution in the reservoirs is:

$$\frac{dV_k}{dt} = n_c \cdot (Q_k - Q_k^0) = n_c \cdot N_{\mathrm{wk}} \tag{9}$$

where Eq. 7 was used. Based on the experimental evidences discussed in the previous section (no solute or solvent diffusion through the membranes due to concentration gradients) J_k and N_{wk} may be computed as [17]:

$$J_c = -J_d = (t_c^+ - t_a^+) \cdot \frac{I}{F} = (t_a^- - t_c^-) \cdot \frac{I}{F} \tag{10}$$

$$N_{\mathrm{wc}} = -N_{\mathrm{wd}} = t_w \cdot \tilde{V} \cdot \frac{I}{F} \tag{11}$$

where t_c^+ and t_a^+ represent, respectively, the transport number of Na^+ in the cation- and in anion-exchange membranes, and t_c^- and t_a^-, analogously, are the transport number of lactate anion in the cation- and in the anion-exchange membranes; t_w is the water transport number in the membranes, and $\tilde{V}$ is the molar volume of water.

The overall stack voltage, E_{tot}, may be written as a sum of several terms:

$$E_{\mathrm{tot}} = E_{\mathrm{el}} + n_c \cdot (IR + E_j + E_D) \tag{12}$$

where E_{el} is the difference between the electrode potentials for anode and cathode processes.

The ohmic potential drop, IR, is established in the bulk of the solutions, E_b, across the boundary layers adjacent to the membrane/solution interfaces, E_{bl}, and across the membranes, E_m:

$$IR = E_b + E_{\mathrm{bl}} + E_m \tag{13}$$

These potential drops, together with the junction potential difference, E_j, arising from the concentration gradient across the boundary layers close to the membranes, and the Donnan potential difference, E_D, due to the different distribution of diffusible ions at the membrane/solution interfaces, may be expressed in terms of the bulk concentrations of the various solutions and the operating parameters of the stack (e.g. the current density) considering the simple model represented in Fig. 11 [16]. Potential gradients are taken as the potential on the right side minus the potentials on the left one (divided by the distance).

The ohmic potential drop in the bulk of the solutions for a single cell results:

$$E_b = \frac{a}{C_d \cdot \Lambda_d} \cdot i + \frac{a}{C_c \cdot \Lambda_c} \cdot i \tag{14}$$

where a is the compartment thickness (assumed much larger than that of the boundary layers) and $(C_k \cdot \Lambda_k)^{-1}$ gives the solution resistivity (Λ_k is the equivalent conductivity); i indicates the current density.

Assuming a linear concentration gradient in the boundary layer, it is possible to integrate the solution resistivity over the boundary layer thickness leading to the following expression for the ohmic potential drop across the boundary layers of a cell [16]:

$$E_{bl} = \frac{B}{t^-} \ln\left(\frac{C_c^{wc}}{C_c} \cdot \frac{C_d}{C_d^{wc}} \right) + \frac{B}{t^+} \cdot \ln\left(\frac{C_c^{wa}}{C_c} \cdot \frac{C_d}{C_d^{wa}} \right) \tag{15}$$

where $B = D \cdot \mathrm{F}/\Lambda$ depends on the solute diffusion coefficient, D, besides the solution equivalent conductivity (both of them are taken constant with C). Moreover, t^+ and t^- are respectively the transport number of Na^+ and lactate anion in the solution, and the superscripts wc and wa refer to the wall concentration close to the cationic and anionic membrane, respectively (see Fig. 11). Membranes are assumed to be ideally selective.

The average ohmic potential drop across the membranes is related to the current density through the ohmic resistance of the membrane, r_m:

$$E_m = r_m \cdot i \tag{16}$$

The overall junction potential difference across the boundary layers for a cell is given by [18]:

$$E_j = \frac{R \cdot T}{F} \cdot (t^- - t^+) \cdot \ln\left(\frac{C_c^{wc}}{C_c^{wa}} \cdot \frac{C_d^{wa}}{C_d^{wc}} \right) \tag{17}$$

where T is the absolute temperature and R the ideal gas constant. All the other symbols retain the aforementioned meanings.

Finally, the overall Donnan potential difference for a cell is given by [18]:

$$E_D = \frac{R \cdot T}{F} \cdot \ln\left(\frac{C_c^{wc}}{C_d^{wc}} \cdot \frac{C_c^{wa}}{C_d^{wa}} \right) \tag{18}$$

These expressions require the knowledge of the solute concentration close to the membranes, C_k^{wa} and C_k^{wc}. Assuming that the boundary layers established are invariant, the wall concentrations can be computed as functions of the bulk concentrations, the current density, the transport number of the ions as well as the mass transfer coefficient, K [17]:

$$C_k^{wa} = C_k \pm (t_a^- - t^-) \cdot \frac{i}{K \cdot F} \tag{19}$$

$$C_k^{wc} = C_k \pm (t_c^+ - t^+) \cdot \frac{i}{K \cdot F} \tag{20}$$

where the signs + and − refer to the concentrated or diluted compartment, respectively.

Given the current density, this is a model involving nine equations., i.e. 5, 7–9 and 12, in the nine unknowns C_c, C_d, Q_c, Q_d, V_c, V_d, C_c^o, C_d^o, and E_{tot}. Several parameters involved in the model can be deduced from the literature [12,19], and they are summarized in Table 3 together with the geometrical dimensions of the stack [20]. Moreover, a few parameters required by the model and not available in literature were tuned in a previous work [16] on independent experiments concerning lactic acid production from sodium lactate solutions. These parameters are: the N_w^+ transport number in the anion/cation-exchange membranes, the water transport number in the membranes, the average electric resistance of the membranes, the mass transfer coefficient from the bulk solution to the membrane, and the difference between the electrode potentials for anode and cathode processes. Note that almost all these parameters could be measured through properly designed experiments. However, in this work they have been considered as adjustable parameters to be tuned on overall experimental data. Moreover, since all these parameter values were tuned on experiments carried out in the same electrodialysis unit used in this work, they are expected to be suitable for simulating the experimental results discussed in the previous section. The only relevant exception is the average membrane resistance, which is known to depend on the kind of solution involved.

The values of transport numbers in the membranes obtained in the previous work [16] ($t_c^+ = 1$ and $t_a^+ = 0$) mean ideal behavior of these membranes. In other words, the membranes are able to operate a perfect separation of opposite charges. As a consequence, the experimental and theoretical numbers of equivalents

Table 3
Model parameter values

Parameter,		Value	
n_c		10	
A (m^2)		0.02	
a (mm)		0.75	
V_{comp} (m^3)		$0.015\cdot10^{-3}$	
$\tilde{V}$ (m^3/mole)		$18\cdot10^{-6}$	
$t^{\pm}$	$t^- = 0.46$		$t^+ = 0.54$
D (m^2/s)		$1.2\cdot10^{-9}$	
t_w (moles/F)		16.3	
$t_m^{\pm}$	$t_a^- = 1$ $t_a^+ = 0$		$t_c^- = 0$ $t_c^+ = 1$
r_m ($\Omega\cdot$cm^2)		18.9	
K (m/s)		10^{-3}	
E_{el} (V)		2.7	

transferred during each run (which can be computed as discussed previously, see Eq. 2) have to be equal each others. As shown in Fig. 12, this is true also for the experiments performed in this work.

The water transport number in the membranes affects the volume variations of the solution in the reservoirs. Since all the runs were carried out at constant current density, Eqs. 9 and 11 can be easily recast in the following one:

$$V_{d,in} - V_d(t) = V_c(t) - V_{c,in} = n_c \cdot t_w \cdot \tilde{V} \cdot \frac{I}{F} \cdot t \qquad (21)$$

where the subscript in refers to the initial conditions.

Also in this case, the comparison between the experimental volume variations in the reservoirs and the predictions of Eq. 21 using the value of t_w estimated in the previous work [16] (t_w = 16.3 mol/F for sodium lactate solution), shows a good agreement (see Fig. 13).

Lastly, using the original values for the three parameters: r_m = 18.9 Ω · cm^2, K = 10^{-3} m/s, E_{el} = 2.7 V, a slight disagreement between measured and predicted overall stack voltage has been found, as shown for the sake of example in Fig. 14 (dashed curve) for run A. Experimental and model results can be easily reconciled by changing the value of the average membrane resistance from 18.9 to 15.2 Ω · cm^2 (Fig. 14, solid curve), without modifying any other parameter value.

Finally, an overall comparison between experimental and model results is reported in Figs. 15 and 16 in terms of the process performance indexes defined by Eqs. 1–4. Also for these quantities, the agreement

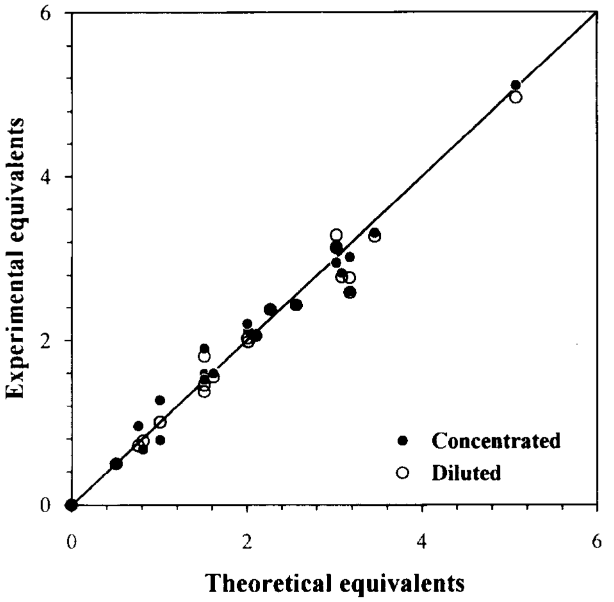

Fig. 12. Comparison between experimental and theoretical numbers of equivalents transferred in all the runs.

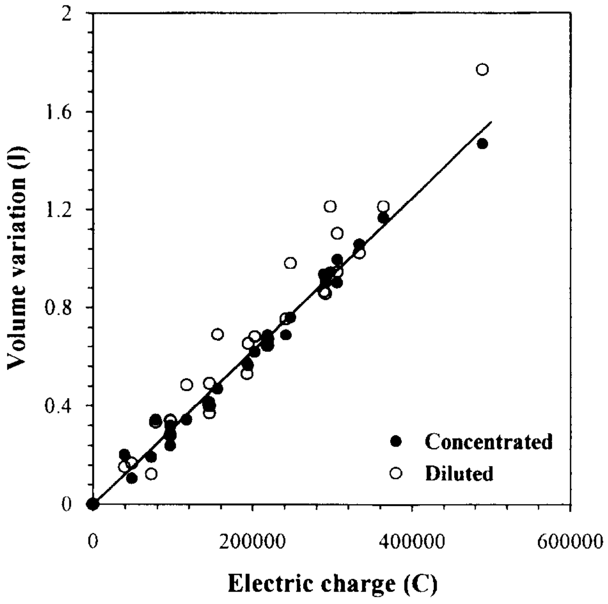

Fig. 13. Comparison between experimental volume variation in the reservoirs (symbols) and model predictions (——) for all the runs.

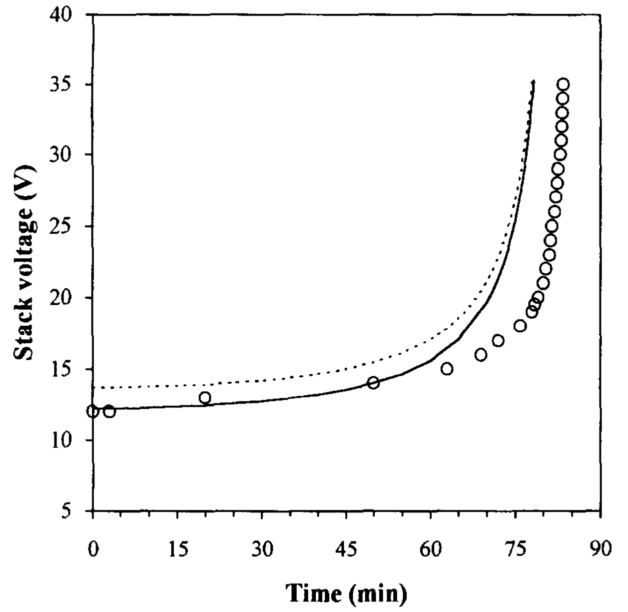

Fig. 14. Comparison between experimental stack voltage (symbols) and model predictions for run A: (– – –) r_m = 18.9 Ω·cm²; (——) r_m = 15.2 Ω·cm². See Table 1 for run label.

between experiments and model results is quite satisfactory.

5. Conclusions

In this work the concentration process of sodium lactate by electrodialysis was investigated. It has been found that commercial anion- and cation-selective membranes are able to operate a nearly perfect separation of opposite charges, resulting in current efficiency values close to 100%. This is true as far as low current density values are considered (that is, up to about 400 A/m²); higher values lower the stack performance. Moreover, water permeation through the membranes due to concentration gradients is negligible for concentration differences across the membrane up to about 90 g/l, and almost all the solute can be recovered in a batch recirculation operation mode for current density values lower than 400 A/m². Increasing the current density results in a reduction of the sodium lactate recovered. Energy-related indexes (i.e. the specific energy requirement and the average power requirement, see Eqs. 3 and 4) do not depend on the initial solution concentration, but they remarkably increase with the current density. However, this also results in a short process time, thus requiring an economic analysis to find the best operating conditions.

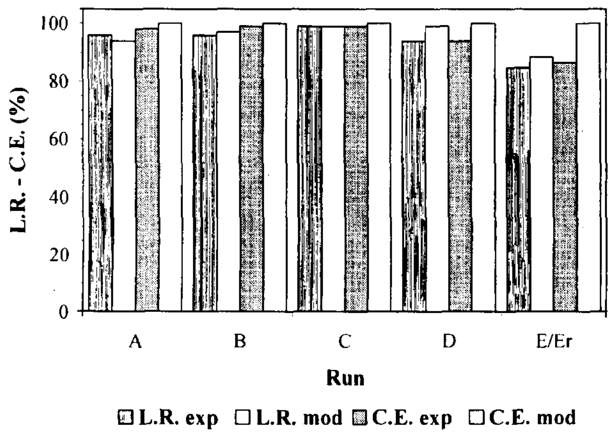

Fig. 15. Process performance indexes: comparison between experimental and model results. Legend as in Fig. 9. See Table 1 for run labels.

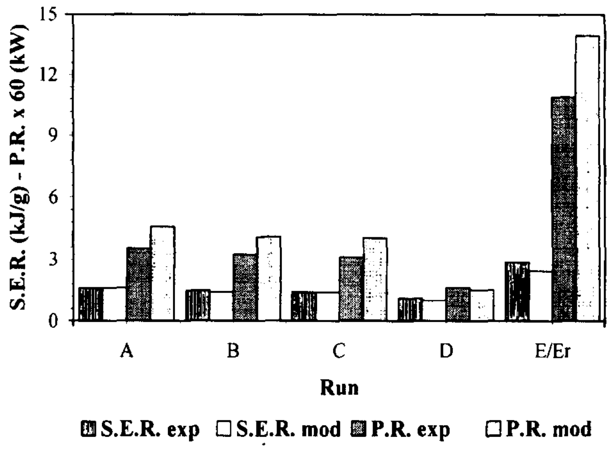

Fig. 16. Process performance indexes: comparison between experimental and model results. Legend as in Fig. 9. See Table 1 for run labels.

Moreover, the reliability of a general mathematical model previously developed was verified for the case under investigation. It has been shown that this model is able to reproduce the experimental findings by tuning only one adjustable parameter, the average membrane resistance, which is known to depend on the solution considered. Since similar results were obtained for a four-compartment unit, this model can be regarded as a suitable tool for designing and optimizing the involved processes. Obviously, different stacks or membranes would require a re-tuning of some parameter values; this can be easily done following the procedure discussed elsewhere [16].

Acknowledgements

Financial support of Sespi s.r.l. to N.B. is gratefully acknowledged.

Notation

A = surface area of each membrane, m²
a = compartment thickness, m
B = $F \cdot D/\Lambda$

C = concentration, eq/m^3 or g/l
C.E. = current efficiency, %
D = diffusion coefficient, m^2/s
E_b = ohmic potential drop across bulk solution, V
E_{bl} = ohmic potential drop across boundary layer, V
E_D = Donnan potential difference, V
E_{el} = difference between the electrode potentials for anode and cathode processes, V
E_j = junction potential difference across boundary layer, V
E_m = ohmic potential drop across membrane, V
E_{tot} = overall stack voltage, V
EW = equivalent weight, g/eq
F = Faraday constant, C/eq
I = current, A
i = current density, A/m^2
IR = ohmic potential drop, V
J = ion flow rate through the membrane, eq/s
K = mass transfer coefficient, m/s
L.R. = sodium lactate recovery, %
N_w = water flow rate through the membrane, m^3/s
n_c = number of cells
NaL = sodium lactate amount, g
P.R. = average power requirement, kW
Q = volumetric flow rate, m^3/s
R = resistance, Ω
R = universal gas constant, J/mole · K
r_m = ohmic resistance of the membranes (for unit cross section), Ω · cm^2
S.E.R. = specific energy requirement, kJ/g
T = absolute temperature, K
t = time, s or min
t^+ = transport number of Na$^+$ in solution
t^- = transport number of lactate anion in solution
t_a^+ = transport number of Na$^+$ in the anion-exchange membrane
t_c^+ = transport number of Na$^+$ in the cation-exchange membrane
t_a^- = transport number of lactate anion in the anion-exchange membrane
t_c^- = transport number of lactate anion in the cation-exchange membrane
t_w = water transport number in the membranes, moles/F
V = volume, m^3 or l
$\tilde{V}$ = water molar volume, m^3/mole

Subscripts

a = anion-selective membrane
c = cation-selective membrane
c = concentrated
comp = compartment
d = diluted
exp = experimental
fin = final
in = initial
k = generic compartment or reservoir, either concentrated or diluted
m = membrane
th = theoretical
w = water

Superscripts

$\pm$ = either cation or anion
o = entering the cell
wa = wall, anion-selective membrane
wc = wall, cation-selective membrane

Greek letters

Δequiv = variation of equivalents (absolute value), eq
δ = boundary layer thickness, m
Λ = equivalent conductivity, S · m^2/eq

References

[1] Sridhar, S. (1988) Application of electrodialysis in the production of malic acid. J. Membrane Sci. 36, 489–495.

[2] Hongo, M., Nomura, Y. and Iwahara, M. (1986) Novel method of lactic acid production by electrodialysis fermentation. Appl. Environ. Microbiol. 52, 314–319.

[3] Nomura, Y., Iwahara, M. and Hongo, M. (1988) Acetic acid production by an electrodialysis fermentation method with a computerized control system. Appl. Environ. Microbiol. 54, 137–142.

[4] Datta, R. (1989) Recovery and purification of lactate salts from whole fermentation broth by electrodialysis. Eur. Pat. Appl. EP 0 338 162 A1.

[5] Kuppinger, F.F., Busch, C. and Eigenberger, G. (1992) Direct electrodialysis of fermentation broth with periodic removal of fouling layers. DECHEMA Biotechnol. Conf. 5, 671–674.

[6] Yao, P. and Toda, K. (1990) Lactic acid production in electrodialysis culture. J. Gen. Appl. Microbiol. 36, 111–125.

[7] Ishizaki, A., Nomura, Y. and Iwahara, M. (1990) Built-in electrodialysis batch culture, a new approach to release of end product inhibition. J. Ferment. Bioeng. 70, 108–113.

[8] Vonktaveesuk, P., Tonokawa, M. and Ishizaki, Y. (1994) Stimulation of the rate of, L-lactate fermentation using, *Lactococcus lactis*, IO-1 by periodic electrodialysis. J. Ferment. Bioeng. 77, 508–512.

[9] Fukuzaki, H., Aiba, Y., Yoshida, M., Asano, M. and Kumakura, M. (1989) Synthesis of biodegradable poly(L-lactic acid-co-D,L-mandelic acid) with relatively low molecular weight. Makromol. Chem. 190, 2407–2415.

[10] Yen, Y.H. (1990) Recovery of lactic acid from fermentation broth by electrodialysis. Ph.D. thesis, University of, Illinois.

[11] Colon, G. (1986) Recovery of lactic acid from fermented acid-cheese whey via electrodialysis. Ph.D. thesis, University of, Massachusetts.

[12] Boniardi, N. (1995) Lactic acid recovery by electrodialysis: experimental tests and mathematical modeling. Ph.D. thesis (in Italian), Politecnico di Milano.

[13] Heriban, V., Skara, J., Sturdik, E. and Ilavski, J. (1993) Isolation of free lactic acid using electrodialysis. Biotechnol. Tech. 7, 63–68.

[14] Glassner, D. and Datta, R. (1990) Process for production and purification of lactic acid. Eur. Pat. Appl. EP 0 393 818 A1.

[15] Boniardi, N., Rota, R., Nano, G. and Mazza, B. (1995) Lactic acid production by electrodialysis. Part, I: Experimental tests. Submitted to J. Appl. Electrochem.

[16] Boniardi, N., Rota, R., Nano, G. and Mazza, B. (1995) Lactic acid production by electrodialysis. Part, II: Modeling. Submitted to J. Appl. Electrochem.

[17] Evangelista, F. (1987) A graphical method for the design of an electrodialysis stack. Desalination 64, 353–365.

[18] Vetter, K.J. (1967) Electrochemical kinetics. New York: Academic Press.

[19] Reid, R.C., Praustnitz, J.M. and Sherwood, T.K. (1977) The properties of gases and liquids. New York: McGraw-Hill.

[20] Eurodia, (1992) Instruction manual of double decomposition electrodialyzer TS-EUR2-5 D, Wissous.